RESEARCH PAPER

Computational Investigation of KRAS regulatory targets through *Berberine chloride* in Lung cancer: Targeting upstream regulators of the MAPK Pathway

Arjun KR[1], Arya V M[2], Ullas Prasanna[3], Baburao Gaddala[4], Shailasree Sekhar[5], Jeyarish V[1], Varshitha BR[1], Vindhya M[1`], Modugapalem Hemalatha[*6], Kanthesh M Basalingappa[*1]

[1*] Division of Molecular Biology, School of Life Sciences, JSS Academy of Higher Education & Research, Mysuru, Karnataka, India

[2]Assistant Professor, Department of Kriya Sharira, JSS Ayurveda Medical College-570028, Mysuru, Karnataka, India
[3]Department Biotechnology, School of Basic & Applied Sciences, Dayananda Sagar University, Innovatio Campus, Bengaluru, Karnataka, India.
[4]Department of Chemical Engineering, School of Studies of Engineering and Technology, Guru Ghasidas Vishwavidyalaya, A Central University, Koni, Bilaspur, Chhattisgarh-495009, India.
[5]Division of Biochemistry, School of Life Sciences, JSS Academy of Higher Education & Research, Mysuru, Karnataka.
[6*]Department of Biotechnology, Sri Venkateswara University, Tirupati-517502, India

Corresponding author(s). Kanthesh M Basalingappa*, Modugapalem Hemalatha
E-mail(s): kantheshmb@jssuni.edu.in ; hemamoduga@gmail.com

ABSTRACT:

The KRAS-driven Lung Adenocarcinoma remains a major therapeutic challenge in the field of Oncology. This is due to the poor drug ability and shallow binding pockets present in the KRAS, which made them undruggable for decades. Due to this, to target the KRAS present in the MAPK pathway, the targeting is being done through an indirect way, i.e., through upstream regulators of KRAS. Based on the literature evidence we focused on targeting the upstream regulators such as SOS1, SHP2, and the chaperone PDE6D. To regulate this, a promising antitumor potential bioactive compound, *Berberine chloride,* was chosen. Despite being well focused target drug, *Berberine's* interaction with KRAS is underexplored. Hence, this was focused on in our paper as a research gap. This will be further carried to wet lab validation in our future research.

Objective: To validate the best binding protein that can be targeted through *Berberine chloride,* to regulate the KRAS mutations using In Silico approaches.

Methods: Ligand structure was obtained using the PubChem database. Protein structures were retrieved using the Protein Data Bank. Docking was performed using Schrodinger software. MD simulations were carried out using Desmond. pkCSM was used to carry out ADMET profiling.

Results: *Berberine chloride* exhibited favourable binding affinities with all the docked upstream regulators of KRAS and chaperone PDE6D. MD simulation, which was carried out after docking, exhibited a stable ligand-protein complex with low structural deviations and persistent interactions throughout the duration of the simulation. The ligand's structural stability and its limitations were also analysed through RMSD and RG analyses. The ADMET profiling resulted in acceptable and drug limitations in some of the subject criteria is to be seriously addressed. This is to be validated through a wet lab in the future.

**Author for Correspondence: kantheshmb@jssuni.edu.in*

Conclusion: The overall results give a clear-cut insight into the future wet lab validation. PDE6D chaperone has shown a better affinity in all the studies, and *Berberine* has exhibited better binding affinity. The ADMET exhibits and shows the limitations of the drug that are to be further addressed in the wet lab. Overall, this data gives a solid foundation for the wet lab mechanistic approaches.

Keywords: KRAS, In-silico, Lung Cancer, Adenocarcinoma, MAPK, *Berberine chloride*.

How to cite this article: Arjun KR, Arya VM, Prasanna U, Gaddala B, Sekhar S, Jeyarish V, Varshitha BR, Vindhya M, Hemalatha M, Basalingappa KM. Computational Investigation of KRAS regulatory targets through Berberine chloride in Lung cancer: Targeting upstream regulators of the MAPK Pathway. Int J Drug Deliv Technol. 2026;16(40s): 100-132. DOI: 10.25258/ijddt.16.40s.13

Graphical Abstract:

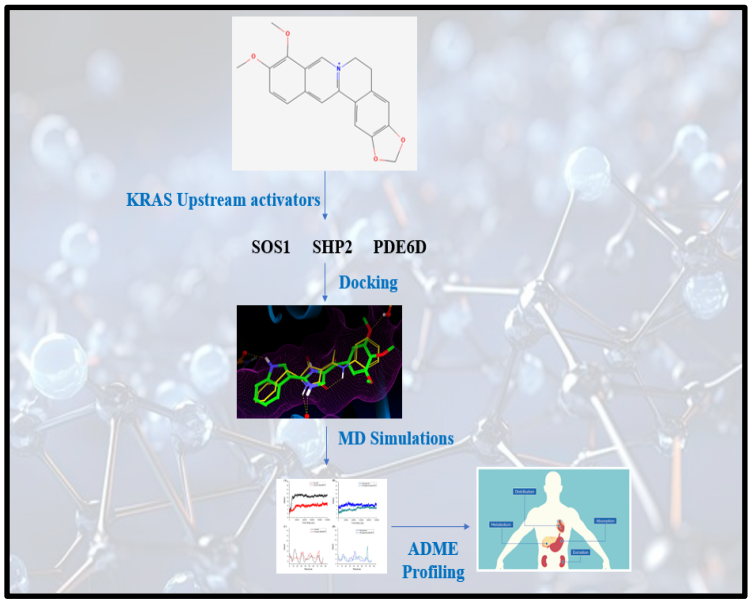

Abbreviations:

1. KRAS- Kirsten Rat Sarcoma Viral Gene
2. NSCLC- Non-Small Cell Lung Cancer
3. LUAD- Lung Adenocarcinoma
4. NRAS- Neuroblastoma Rat Sarcoma Viral Oncogene
5. HRAS- Harvey Rat Sarcoma Viral Gene
6. GTP- Guanosine Triphosphate
7. GDP- Guanosine Diphosphate
8. GAPs- GTPase-activating proteins
9. MAPK- Mitogen-Activated Protein Kinase
10. ERK- Extracellular Signal-Regulated Kinase
11. EGF- Epidermal Growth Factor
12. EGFR- Epidermal Growth Factor Receptor
13. FTIs- Farnesyl Transferase Inhibitors

14. SOS1- Son of Sevenless homolog 1
15. SHP2- Src Homology 2 domain-containing protein tyrosine phosphatase 2
16. ECOG- Eastern Cooperative Oncology Group
17. PDE6D- Phosphodiesterase 6 Subunit Delta
18. RTK- Receptor Tyrosine Kinase

Introduction:

Non-small cell lung cancer (NSCLC) is the most common kind of lung cancer and the primary cause of cancer-related deaths globally. One of the most prevalent and thoroughly researched histological subtypes is lung adenocarcinoma (LUAD). Over the last decade, the development and authorization of immune checkpoint inhibitors and targeted medications have significantly enhanced treatment options and improved patient outcomes, complementing standard therapeutic approaches such as surgery, radiation, and chemotherapy. However, therapy results still vary in a broad range, even with the individualized treatment alternatives offered. Thus, recognizing the importance of genetic co-alterations and their impact on treatment responses is crucial, among other things. Kirsten rat sarcoma viral oncogene homolog, or KRAS, is important for the initiation and spread of many malignancies, including non-small cell lung cancer. Approximately 25% of cases have mutations that constitutively activate KRAS signaling pathways, promoting unchecked cell growth and survival [1,2].

The deregulation of the mitogen-activated protein kinase/extracellular signal-regulated kinase (MAPK/ERK) signaling pathway in cancers is caused by a variety of biomolecular alterations. Lung cancer is among the many malignancies that have been linked to overexpression of epidermal growth factor (EGF), EGF receptor (EGFR), as well as activating mutations in its intracellular kinase domains. Intermediaries that transfer EGFR signals to rat sarcoma virus (RAS) proteins include growth factor receptor binding proteins, son-of-sevenless (SOS), and a guanine nucleotide exchange factor (GEF) [3-4]. The three RAS genes' proteins—Kirsten RAS (KRAS), neuroblastoma RAS (NRAS), and Harvey RAS (HRAS)—transmit extracellular signals from membrane-bound receptors to downstream mediators and effectors [5]. About 33% of human neoplasms are caused by activating mutations affecting all the RAS genes, which have been found in malignancies. 86% of instances of mutant RAS are caused by KRAS mutations, which are by far the most prevalent. The frequency of KRAS mutations in Black and White Americans is comparable. RAS proteins belong to the G-protein superfamily of proteins that bind guanine nucleotides. They function as molecular switches, switching between the active GTP-bound and the inactive GDP-bound states. The intrinsic GTPase activity mediated by GTPase-activating proteins (GAPs) stops signaling in the active states [6-7].

Until recently, cancers caused by mutated RAS proteins were thought to be incurable. Because of the micromolar amounts of GTP in cells and its picomolar dissociation constants from RAS proteins, it has long been difficult to design compounds that can competitively displace GTP from RAS. Since the C-terminal farnesyl cysteine was shown to be crucial for RAS membrane localization and function, previous attempts to create anti-RAS medications focused on the manufacture of farnesylation inhibitors. However, geranylgeranylation was developed to circumvent the effects of farnesyl transferase inhibitors (FTIs), making success with this

strategy challenging. The FTIs were also quite hazardous. The creation of kinase inhibitors that target the downstream mediators of RAS signaling, including RAF, MEK1/2, and ERK1/2, was an indirect and slightly more effective approach to addressing the RAS dilemma. In order to allosterically limit and disrupt oncogenic signaling, chemists have lately been designing small compounds that fit into tiny nooks on KRAS. These chemicals target certain mutant RAS protein subsets and react chemically with them [8-10].

The previous literature evidence shows that direct targeting of KRAS mutations has been drugged with Adgarasib and Sortarasib effectively. So, with these evidences, we focused on targeting this target indirectly using a less-toxic bioactive compound, *Berberine chloride*. Before taking it into the wet lab validation, we intended to validate it through an in-silico approach. To date, the research evidence shows up for sub-mutations of a few KRAS, such as G12C and G12S. But it still goes on with clinical trials.

In this study, we clearly address the research gap of targeting the chaperone PDE6D and upstream regulators SOS1 and SHP2 through literature evidence. The MAPK pathway was selected based on confirmation with the KEGG database.

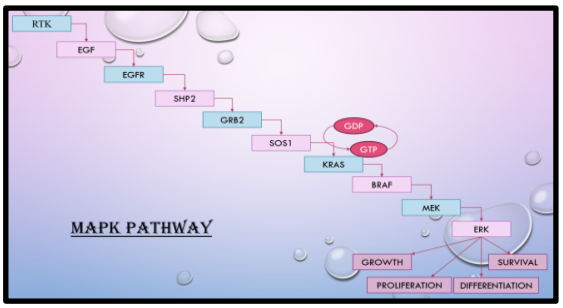

Figure 01: Canonical representation of the MAPK pathway.

Based on this reference MAPK pathway, KRAS was targeted. As it cannot be targeted directly, due to its shallow pocket, the upstream indirect targets were chosen, such as SOS1, SHP2, and the chaperone PDE6D.

Introduction to *Berberine chloride*:

Chemotherapy, immunotherapy, targeted treatment, radiation therapy, and surgical lung tumor excision are now used to treat lung cancer [11]. The main disadvantages of the synthetic drug compounds now on the market for chemotherapy are their low bioavailability and off-target effects. On the other hand, phytoconstituents produced from natural products are becoming more and more popular as a potential therapy target for LC. The stems, bark, and roots of plants of the genus Berberis contain large amounts of berberine, an isoquinoline alkaloid that is well-known for its anti-cancer and anti-inflammatory qualities [12-13]. It has been demonstrated that berberine inhibits the development of non-small cell lung cancer (NSCLC) by repressing DNA repair and replication, inducing apoptosis, and inhibiting proliferation and colony formation ability [14]. The main disadvantages of berberine and many other plant-derived active

principles include poor bioavailability and restricted bio-absorption, which restrict their in vivo efficacy and therapeutic application despite their promising anti-cancer activity and immense potential [15-16]. The absence of efficient detection and treatment methods is one of the main causes of the rising number of lung cancer occurrences. Controlling carcinogenesis and metastasis may be facilitated by understanding the molecular processes underlying lung cancer pathogenesis and developing methods to block specific pathways at the molecular level [17].

Based on this literature evidence, *Berberine chloride*, which is a promising anti-cancerous phyto constituent, was used as the drug of interest in our study. As KRAS-mutated non-small cell lung cancer is the most mutated oncogenic driver, though its mechanism is well known, the therapeutic strategy for this protein is still underexplored.

KRAS-Mutated Lung Cancer Incidence:

The total prevalence of RAS gene mutations was 22.58%, with KRAS mutations being the most common and frequent kind, according to data on RAS mutations in 17,993 cancer cases [18]. Most KRAS mutations occur at codons 12 and 13 of exon 2 and 61 of exon 3. Codon 12 substitution mutations (purine is transformed to pyrimidine or vice versa), G12C (39%), and G12V (18–21%) are the most prevalent mutation subtypes in KRAS-mutant lung cancer. G12D (14–18%), G12A (10–11%), and transition mutations (purine being substituted by purine or pyrimidine by pyrimidine) come next.

G12C is the most common mutation in smokers (45%), whereas G12D is the most common mutation in nonsmokers (46%) [19]. Furthermore, the prevalence of KRAS varies according to the race of the patient (more prevalent in white people than in Asians). According to *Lee et al*.'s analysis of a multicenter retrospective cohort study of 216 Asian KRAS-mutant NSCLC patients, the Eastern Cooperative Oncology Group (ECOG) physical status scores were mostly 0–1 (92.1%), the majority of patients were male (70.8%), the histological subtypes included adenocarcinoma (89.8%), squamous cell carcinoma (4.2%), and others (6.0%), and KRASG12D was the most common subtype (25.5%), mostly in never-smokers, suggesting that factors other than smoking may be the cause of KRAS-mutant lung cancer in Asian patients [20].

1. **Molecular Connectivity of KRAS with the targeted Biomarkers:**

   The research is the basic foundation of in-silico analysis and needs understanding for the connectivity to the proposed research directions. It's important to introduce all the checkpoints leading to the research conducted.

   3.1. KRAS-SOS1 molecular inhibition

   KRAS-SOS1 inhibition of the guanine nucleotide exchange factor (GEF) activity of SOS1, which stimulates GDP-to-GTP exchange on KRAS, traps the oncoprotein in its inactivated GDP-bound form. Small-molecule inhibitors such as BI-3406 and BAY-293 interact with the CDC25 domain of SOS1 instead of interacting with the catalytic interface between the switch I/II regions of

KRAS and inhibit allosteric activation. These agents utilize a shallow pocket that develops around SOS1 residues and KRAS, in which any single-atom rearrangements cause a shift between activation and potent inhibition (IC50 -5 nM) [21].

Orthosteric inhibitors also bind the SOS1-KRAS binding site and stabilize an abortive complex, which prevents the release of nucleotide, but does not result in dissociation. Simulation of atomic interactions shows that GDP extraction occurs in discrete cycles, with the initial step being the docking of the helix of SOS1 to KRAS switch II, and the subsequent steps being the prying of GDP through hydrophobic clashes, which are blocked by inhibitors through rigidification of switch conformations. The potency of Allosteric SOS1 modulators is further increased by conformational clamping, which reduces KRAS-GTP in cells by more than 90 percent and inhibits MAPK rebounding [22-23].

Inhibitors bind to SOS1 E332 and KRAS T35 to form H-bonds to imitate GDP and avoid hydrolysis. This prevents downstream recruitment of RAF and ERK phosphorylation and proliferation in KRAS-mutant NSCLC/CRC cells, synergizing with G12C covalent inhibitors by inhibiting wild-type RAS activation. Preclinical evidence shows that SOS1-KRAS antagonists induce overcoming resistance in tumors with over 80% regression in PDX models [21, 24].

3.2. KRAS-SHP2 molecular inhibition:

SHP2 (PTPN11) is an example of a non-receptor tyrosine phosphatase that activates KRAS signaling by acting upstream (dephosphorylating RTK adaptors, e.g., GRB2) to allow SOS1 to recruit and then GDP-GTP exchange KRAS. Allosteric SHP2 inhibitors interact with a helix of the PTP domain, stabilizing an auto-inhibited conformation that closes the catalytic site, inhibiting p-ERK in KRAS-mutant cells more than 70% [25].

These agents disrupt SHP2-KSR1 scaffolding, repressing adaptive MAPK activation upon MEK inhibition in KRAS-mutant gastric cancer through KSR1 stimulation inhibition. SHP2 inhibition in KRAS G12C tumors augments GDP-locked occupancy of KRAS, which boosts the efficacy of covalent inhibitors (e.g., sotorasib) by inhibiting RTK feedback and wild-type RAS cycling. Dimers can be inhibited by structural clamping of the allosteric site to prevent upstream activation of RAS regardless of the mutant allele [26].

SHP2 blockade, which combats KRAS, has been shown to synergize with KRAS G12C in preclinical models, which induces over 90 percent tumor regression in PDXs of PDAC versus NSCLC. Phase III trials (e.g., KRAS G12C + SHP2 by Jacobio) verify PFS in NSCLC, which extends despite resistance in the KRAS-amplified GEAs. This makes the SHP2 inhibition a crucial approach towards MAPK inhibition in 30% of KRAS-driven cancers [27-28].

3.3. KRAS-PDE6D molecular inhibition:

The prenyl-binding chaperone PDE6D (PDE6D) solubilizes farnesylated KRAS in the cytosol and releases the molecule to RAS/RAF activation in the plasma membrane by shuttling it out of the recycling endosomes. Inhibition interferes with KRAS membrane localization by stabilizing it in PDE6D complexes or preventing access to the prenyl pocket and directing oncogenic KRAS into

cytoplasm/primary cilia and inhibiting ERK signaling [29].

Hydrophobic small molecule inhibitors such as deltarasin bind to the hydrophobic pocket of PDE6D (residues 60-87) and maintain farnesyl-KRAS in high affinity (IC50 -150 nM) and inhibit membrane trafficking. New stabilizers exploit KRAS mutations (e.g., G12V, S3I1) to stimulate PDE6D binding, thereby redressing the balance towards cytoplasmic sequestration and preventing proliferation in KRAS-mutant CRC/PDAC cells. Sophisticated agents such as Deltaflexin3 are combined with sildenafil to enhance solubility/potency, which deactivate p-ERK/S6 by approximately 28% through selective KRAS displacement [30-32].

Crystal structures reveal that inhibitors form π-stacking and H-bonds at the prenyl site. Inhibitors interacting with the prenyl site prevent KRAS release but not PDE6D-wild. PDE6D blockade specifically inhibits viability/growth in KRAS-mutant CRC/NSCLC/PDAC lines, associated with oncogenic levels of KRAS, and in combination with NAMPT blockers reduces tumors. This confirms that PDE6D is a surrogate endpoint of 30% cancers driven by KRAS [33].

Our hypothesis states that "*Berberine chloride* (CID:12356), a bioactive drug, can modulate the KRAS-driven oncogenic signalling in lung adenocarcinoma, inhibiting with stable binding affinity towards the key upstream regulatory proteins (SOS1, SHP2, and chaperone PDE6D) of the MAPK signalling pathway". In this context, targeting KRAS using its chaperone, i.e., PDE6D, is a novel therapeutic strategy. The in-silico approaches based on targeting PDE6D using *Berberine chloride* give the novelty in this paper. The proof or review of literature has been studied in the following sections to understand the connectivity, novelty, and the research gap leading to the research conducted.

4. Objectives:

1. To check the binding affinity of the drug *Berberine chloride* and the upstream regulators of KRAS using Schrodinger.
2. To use Desmond software for 100ns MD simulations to verify the structural stability of the chosen protein-ligand complexes.
3. ADMET profile evaluation of *Berberine chloride* using pkCSM software.

5. Materials and Methods:

5.1. Selection of KRAS upstream targets:

The upstream key regulators were selected based on extensive literature evidence, and to confirm, KEGG pathway analysis was used. The three primary protein targets involved in KRAS activation and signal propagation-SOS1, SHP2, and PDE6D were included for computational evaluation.

5.2. Protein structures Retrieval and Preparation:

Selected proteins' three-dimensional structures were obtained from the Protein Data Bank (PDB). using PubMed literature searches. Proteins were imported into the Schrodinger Maestro workspace and prepared using the Protein Preparation Wizard [34-36].

Preparations included:

- Bond order assignment
- Addition of missing Hydrogen bonds
- Protonation state optimization at pH 7.0
- Removal of water molecules
- Energy minimization

The selection of these KRAS upstream targets was obtained from the Protein Data Bank [34-36].

a. Chain selection (If there are 2 chains in the protein, one chain is selected as the protein structure can have more than one chain [if duplicate chains are found, then only one chain is retained and the other is eliminated]).

b. The General Resolution parameter is less than 2.5 Angstroms. Our selected protein structure resolution is as mentioned in **Table 01**. respectively. The lower the resolution better the quality, and the structure is more meaningful. The resolution of the selected protein structures are as follows:

Sl. No	Name of the Protein	PDB ID	Resolution (A)
1.	SOS1	6SFR	2.5
2.	SHP2	4JEG	1.8
3.	PDE6D	5ML2	2.15

Table 01: Details of the target proteins and their PDB ID.

5.3. Preparation of Ligand:

Berberine chloride's chemical structure was acquired in SDF format from the PubChem database [37]. The ligand was prepared using LigPrep [38].

The Ligand information is as follows:

- Compound name: *Berberine chloride*
- SMILES: COc1ccc2cc3[n+](cc2c1OC)CCc1cc2c(cc1-3)OCO2
- PDB Name: BER
- Pub chem ID: 12456
- Atomic mass: 336.371 au
- Charge: +1
- Molecular Formula: C20H18NO4
- No. of Fragments: 1
- No. of Rot. Bonds: 2

Counter Ion/Salt Information:

Type	Number	Concentration [mM]	Charge
Sodium	8	57.041	+8
Chloride	7	49.911	-7

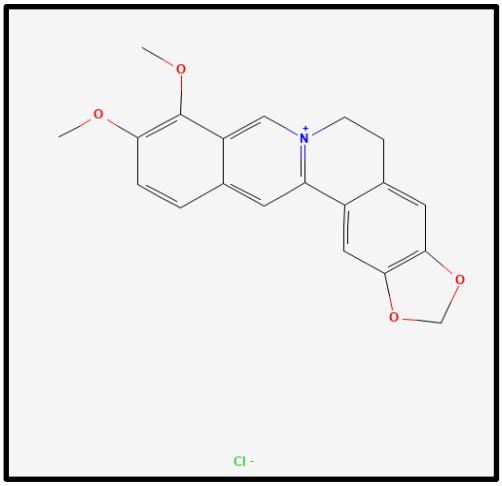

Figure 02: 2D chemical structure of *Berberine chloride*.

5.4. Molecular docking to examine the interaction between proteins and ligands:

Molecular docking was carried out with Schrodinger's Glide module [39].

Grid Preparation:

For grid preparation, the active site literature served as the primary source of evidence [40].

Docking procedure:

Standard precision docking was performed for initial screening.

The top-ranked poses were selected based on their glidescore, interaction stability, and hydrogen-bonding patterns.

5.5. Molecular Dynamics Simulations:

MD simulations were carried out using the Desmond module [41].

Simulation Parameters:

- Simulation Time: 100 ns
- Ensemble: NPT
- Thermostat: Nose-Hoover chain
- Barostat: Martyna-Tobias-Klein
- Time step: 2 fs
- Trajectory recording: 10 ps

Analysis done using MD:

- RMSD- Root Mean Square Deviation
- Protein Ligand Interactions
- Binding Stability over time
- Ligand Stability and its properties, such as SASA, Rg, and others.

5.6. ADMET Prediction:

To check the pharmacokinetic and drug likeness properties, pkCSM software was used [42].

The parameters assessed are as follows:

- Lipinski's rule of Five
- GI absorption
- Water Solubility
- P-gp substrate
- Cytochrome P450 inhibition
- Bioavailability Radar

6. Results and Discussion:

*Author for Correspondence: kantheshmb@jssuni.edu.in

6.1. Docking results:

The docking results are presented in **Table 02** for all the selected proteins.

Sl. No	Name of the Protein	PDB ID	Docking Scores
1.	SOS1	6SFR	-3.4
2.	SHP2	4JEG	-4.8
3.	PDE6D	5ML2	-7.9

Table 02: Representation of the obtained docking score data.

The proteins were subjected to MD simulations for further precision.

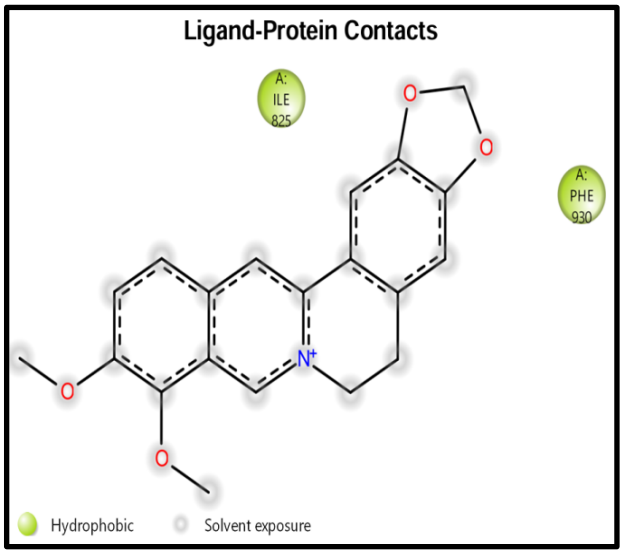

Figure 03: 2D imaging of Ligand-Protein Contacts for SOS1 (6SFR).

The above image, **Figure 03**, represents the protein ligand interaction of *Berberine chloride* with the target protein SOS1 (6SFR). This image gives a representation of hydrophobic interaction and solvent exposure. The docking score is -3.4, which is not a better binding score. Hence, this is to be subjected to MD simulations to check its binding stability. Isoleucine and Phenylalanine are the two amino acids that this protein binds to the ligand.

Figure 04 represents the strong binding between *Berberine chloride* and the target protein chaperone PDE6D (5ML2). The amino acids Isoleucine, Glutamine, and Tryptophan bind with the Ligand to form stability. This binding combination has the highest docking score with -7.9, which can be considered as the better score for taking it further for wet lab validation. It was taken for MD for further analysis.

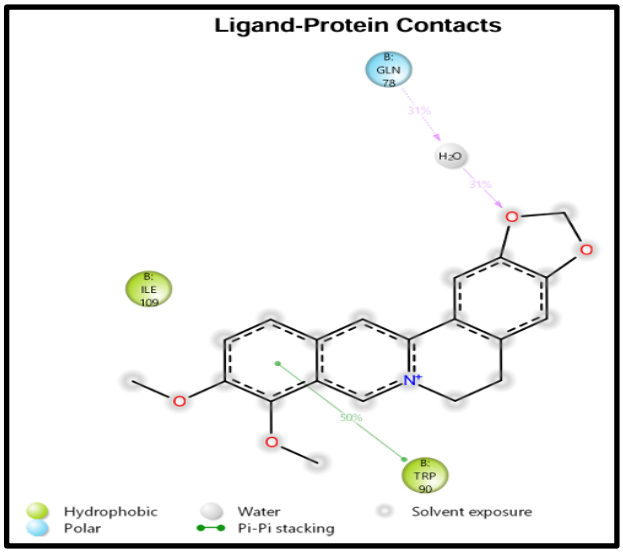

Figure 04: 2D imaging of Ligand-Protein Contacts for PDE6D (5ML2).

The **Figure 05**. represents the 2D imaging of Ligand protein interaction between SHP 2 and *Berberine chloride*. This exhibits low binding affinity due to the compact allosteric pocket of SHP2. As docking suggests limited direct inhibition, it was subjected to MD simulations to check for the transient stabilization due to the conformational adjustments.

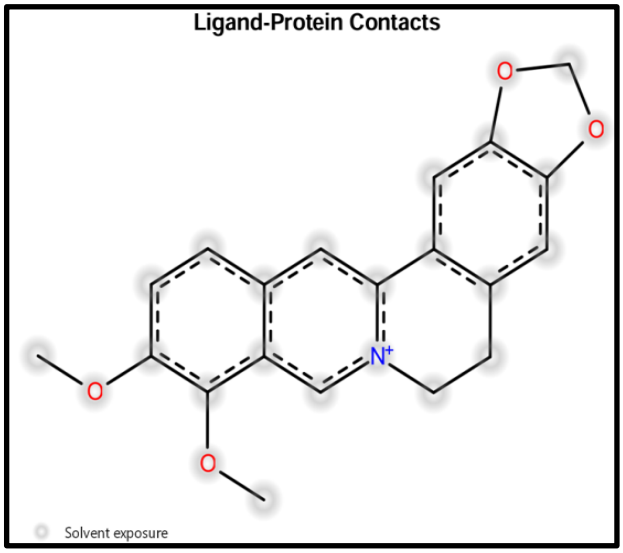

Figure 05: 2D imaging of Ligand-Protein Contacts for SHP2 (4JEG).

As we considered only 3 protein structures for analysis. In spite of getting low docking score we tend to check for its stability hence subjected it for MD simulations.

6.2. Molecular Dynamics (MD) Simulations Result:

6.2.1. Protein Structure Simulation:

The structural properties were aligned with stable parameters for simulation, and MD studies were subjected to 100 ns.

6.2.1.1. Protein Structure Information of SOS1 (6SFR):

Tot. Residues	Prot. Chains	Res. In Chains	No. of Atoms	No. of Heavy Atoms	Charge
480	'A'	ict_values [480]	7964	3973	0

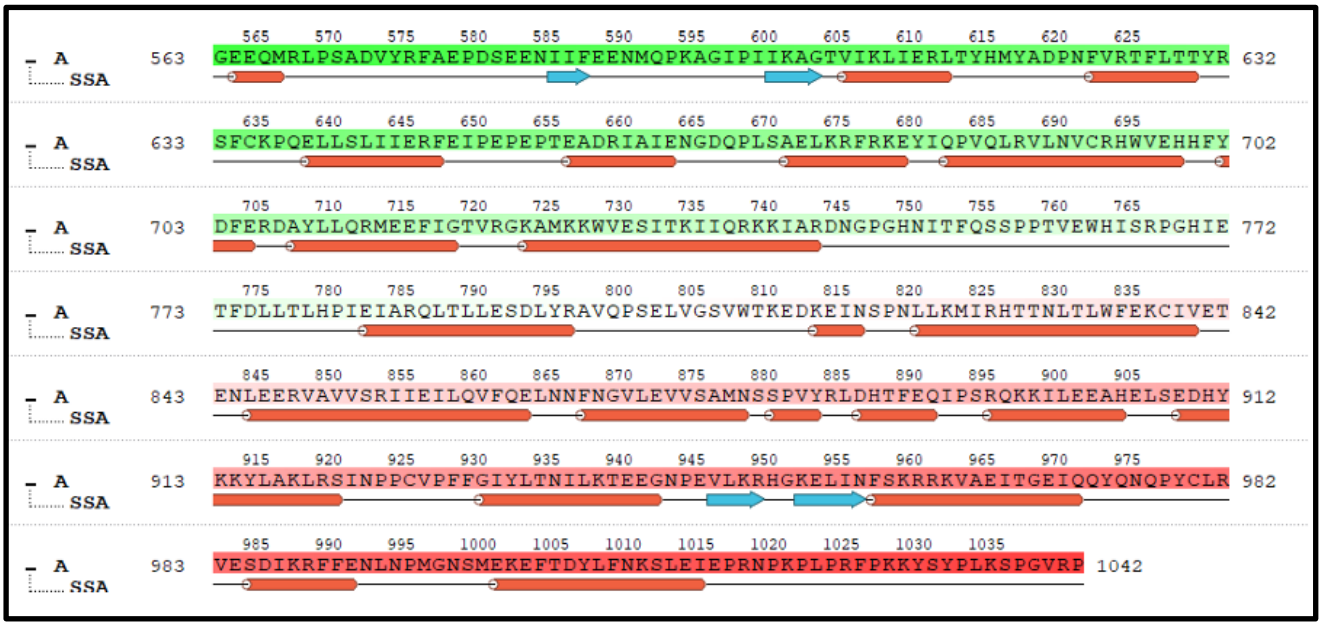

Figure 06: Amino acid Sequence of the protein SOS1 (6SFR)- Chain A.

6.2.1.2. Protein Structure Information of PDE6D (5ML2):

Tot. Residues	Prot. Chains	Res. In Chains	No. of Atoms	No. of Heavy Atoms	Charge
144	'B'	ict_values [144]	2366	1181	0

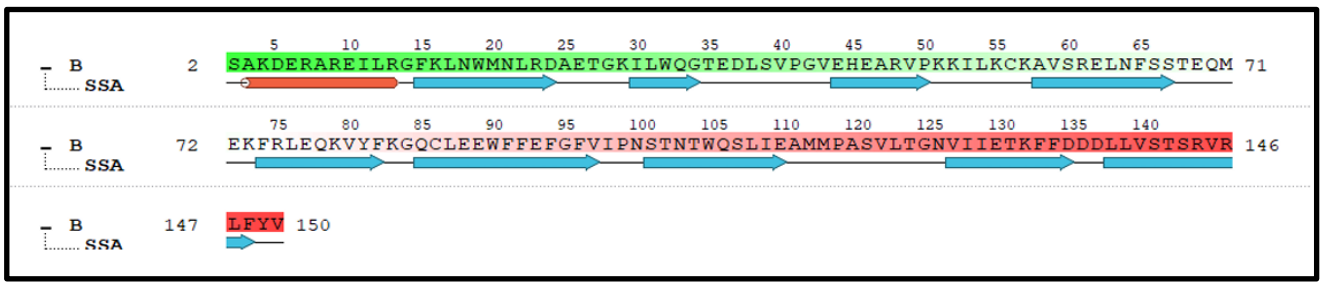

Figure 07: Amino acid Sequence of the protein PDE6D (5ML2)- Chain B.

6.2.1.3. Protein Structure Information of SHP2 (4JEG):

Tot. Residues	Prot. Chains	Res. In Chains	No. of Atoms	No. of Heavy Atoms	Charge
118	'A'	ict_values [118]	1840	928	-2

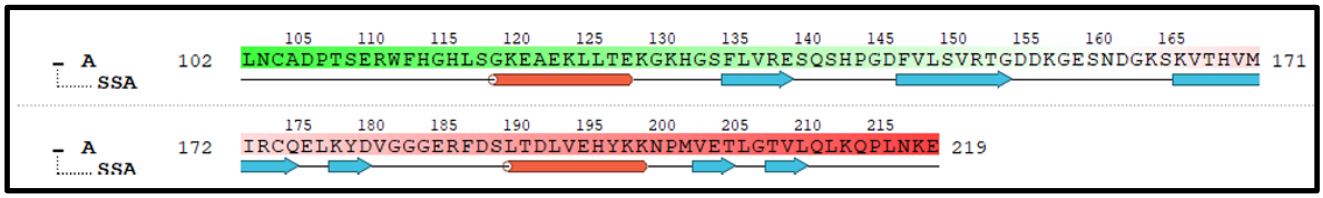

Figure 08: Amino acid Sequence of the protein SHP2 (4JEG)- Chain A.

6.2.2. Protein Ligand RMSD:

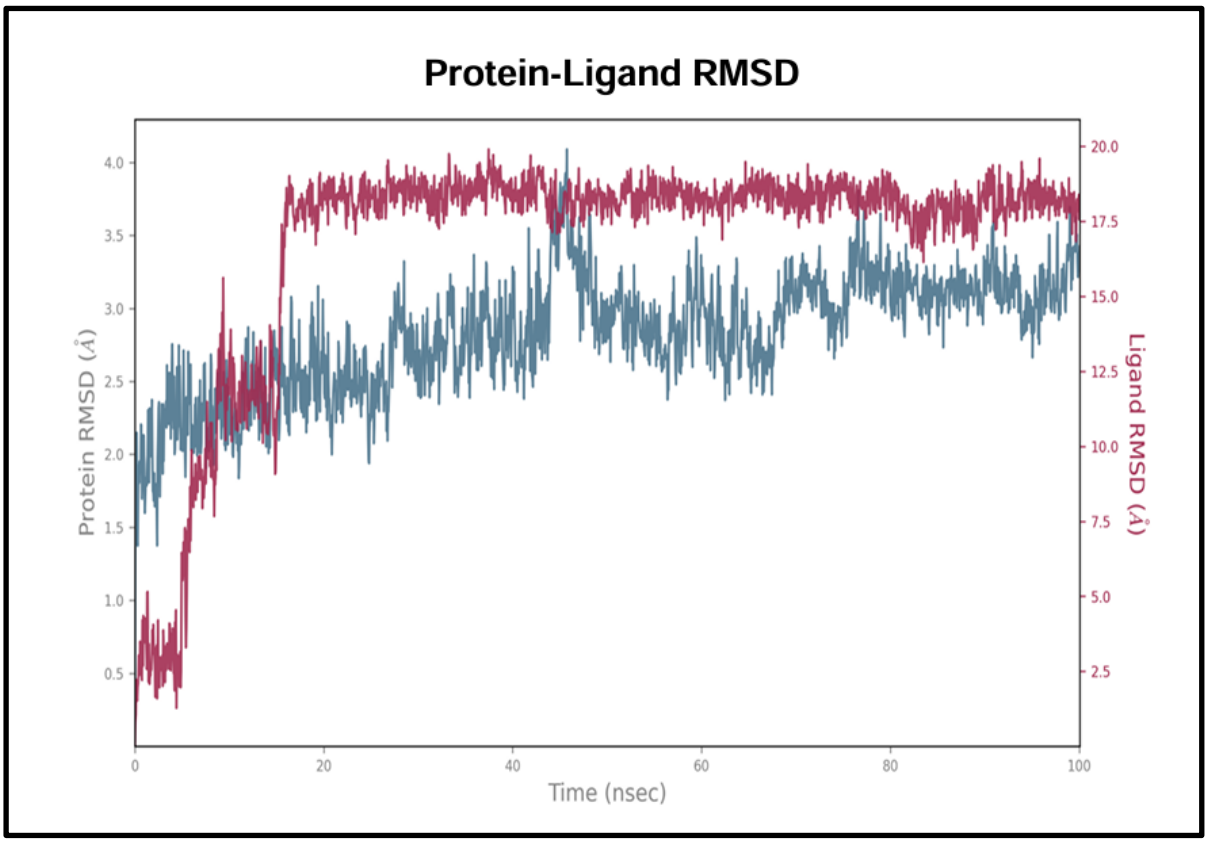

Figure 09: Protein-Ligand RMSD Result of SOS1 (6SFR).

The **Figure 09**. represents the RMSD fluctuations between SOS1 and *Berberine chloride*. The initial fluctuations of RMSD occur up to 40 ns, then the complex stabilizes, which confirms the moderate binding strength predicted by docking. The ligand remains associated with the protein, but it does not exhibit strong conformational restriction.

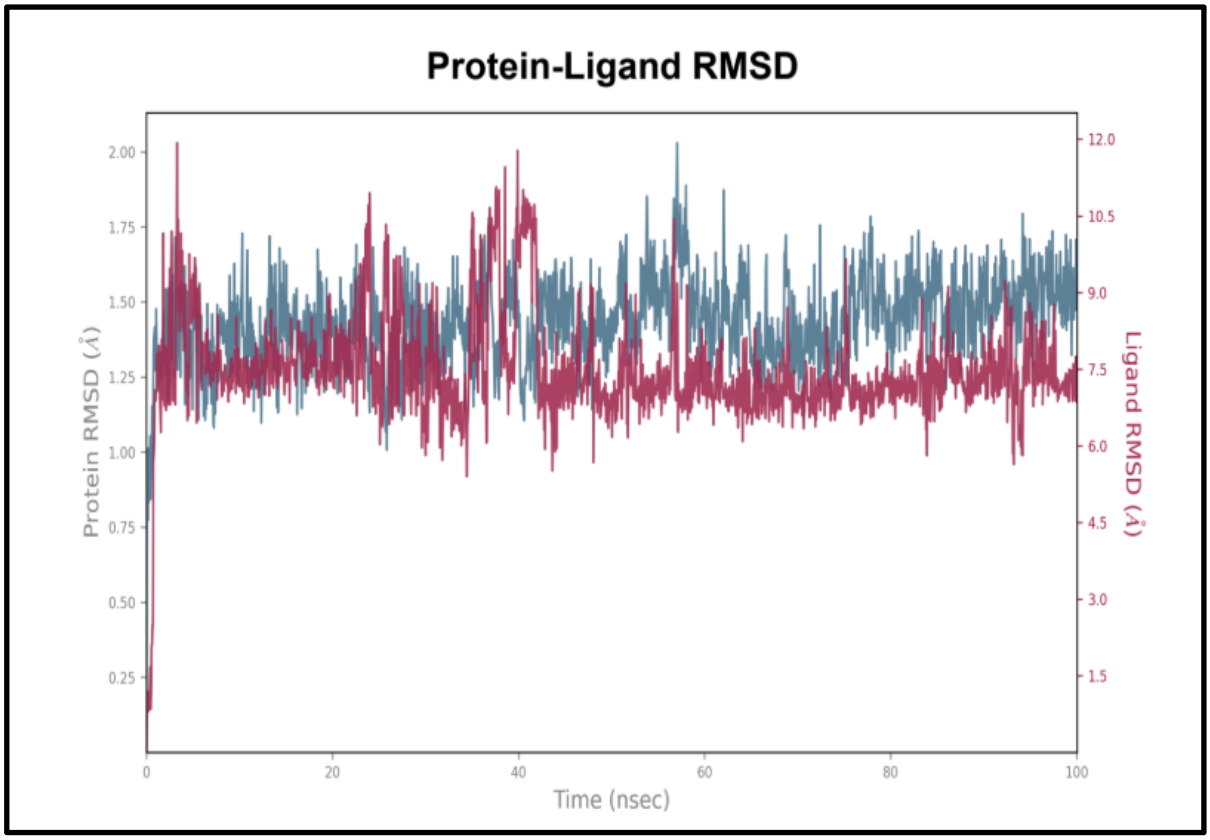

Figure 10: Protein-Ligand RMSD Result of PDE6D (5ML2).

The **Figure 10**. represents the MD simulation RMSD fluctuations between the ligand *Berberine chloride* and the protein PDE6D. This exhibits a stable binding through 100 ns with minimal deviation in some of the time durations. This reflects high structural stability and confirms this target as the most reliable target for *Berberine chloride.*

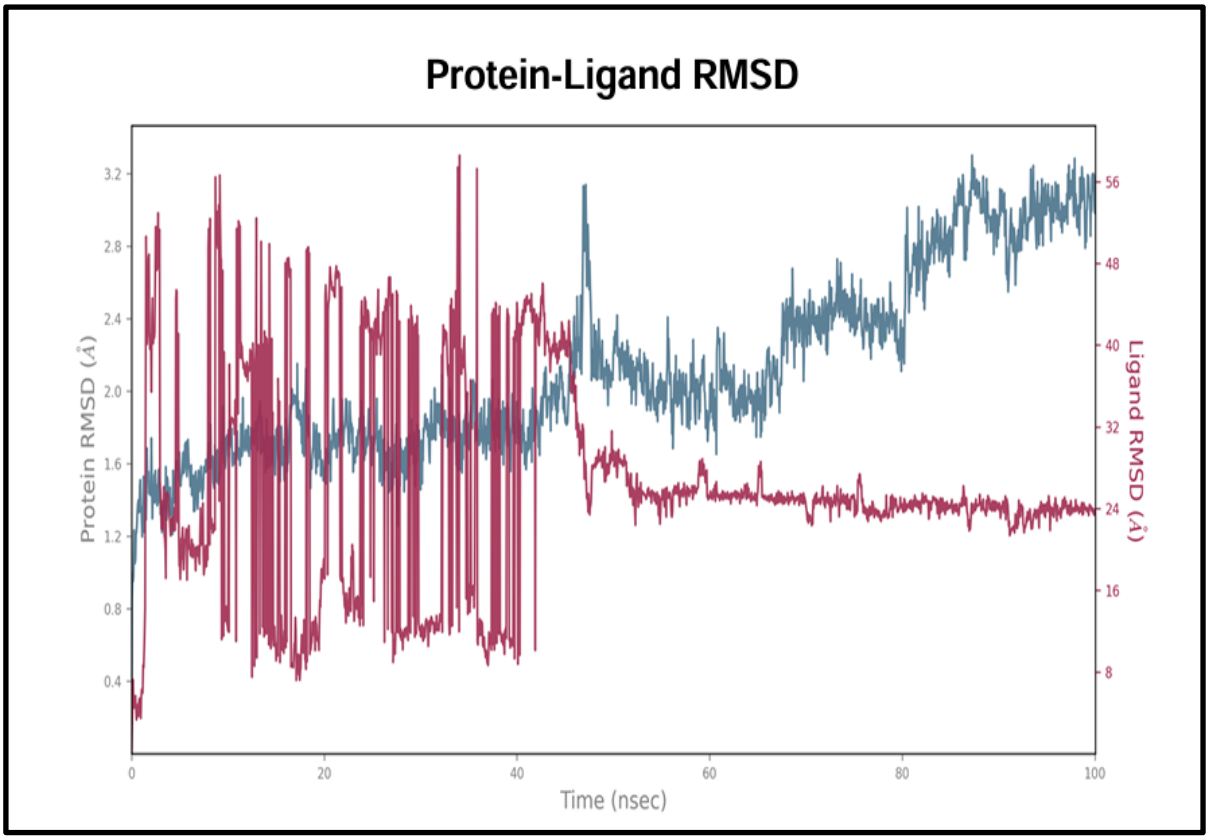

Figure 11: Protein-Ligand RMSD Result of SHP2 (4JEG).

The **Figure 11**. represents the RMSD fluctuations between *Berberine chloride* and SHP2. There is a mild fluctuation exhibited with no major drift. This indicates stable binding but not deeply anchored interactions, with weak docking affinity.

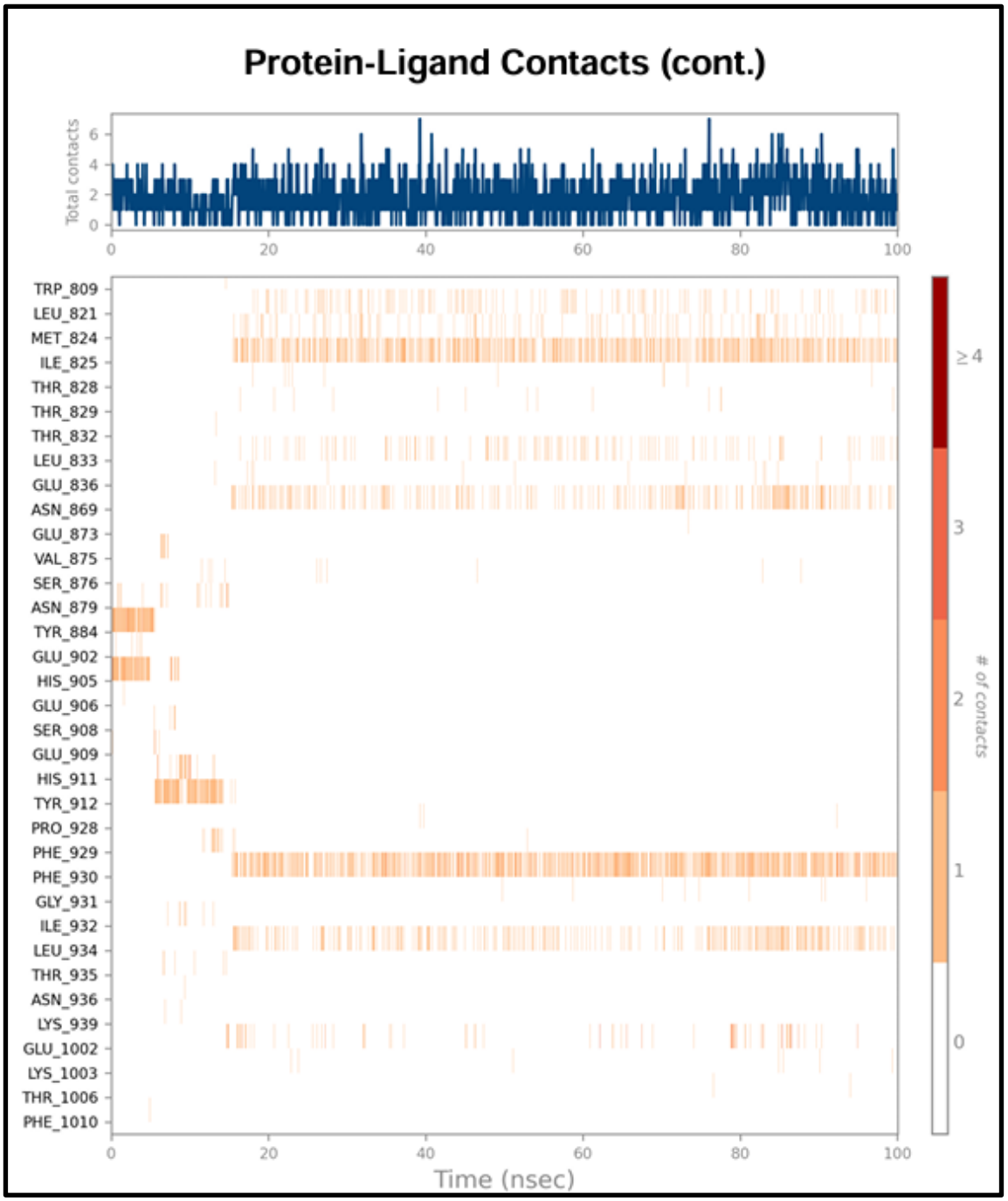

Figure 12: Protein Ligand Contacts of SOS1 (6SFR).

Figure 12. represents the amino acid interaction between the protein SOS1 and the ligand *Berberine chloride*. This shows sparse hydrophobic interactions with short-lived contacts, which indicates weak inhibition potential.

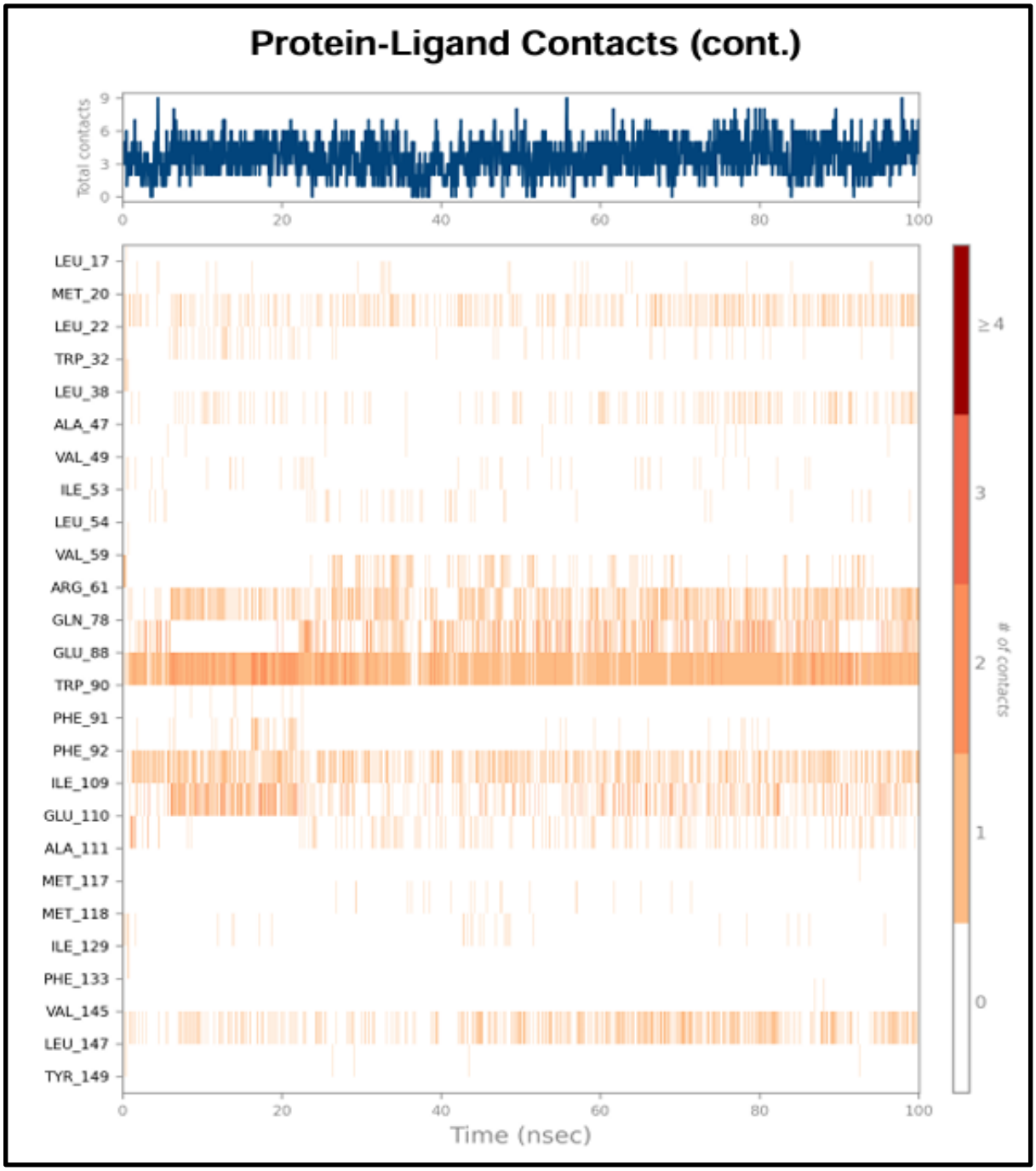

Figure 13: Protein Ligand Contacts of PDE6D (5ML2).

Figure 13. represents the information on amino acid interactions between *Berberine chloride* and PDE6D that exhibits strong and long-lasting interactions with the key residues Tryptophan, Glutamine, and Isoleucine. This confirms a strong binding and high likelihood of functional inhibition.

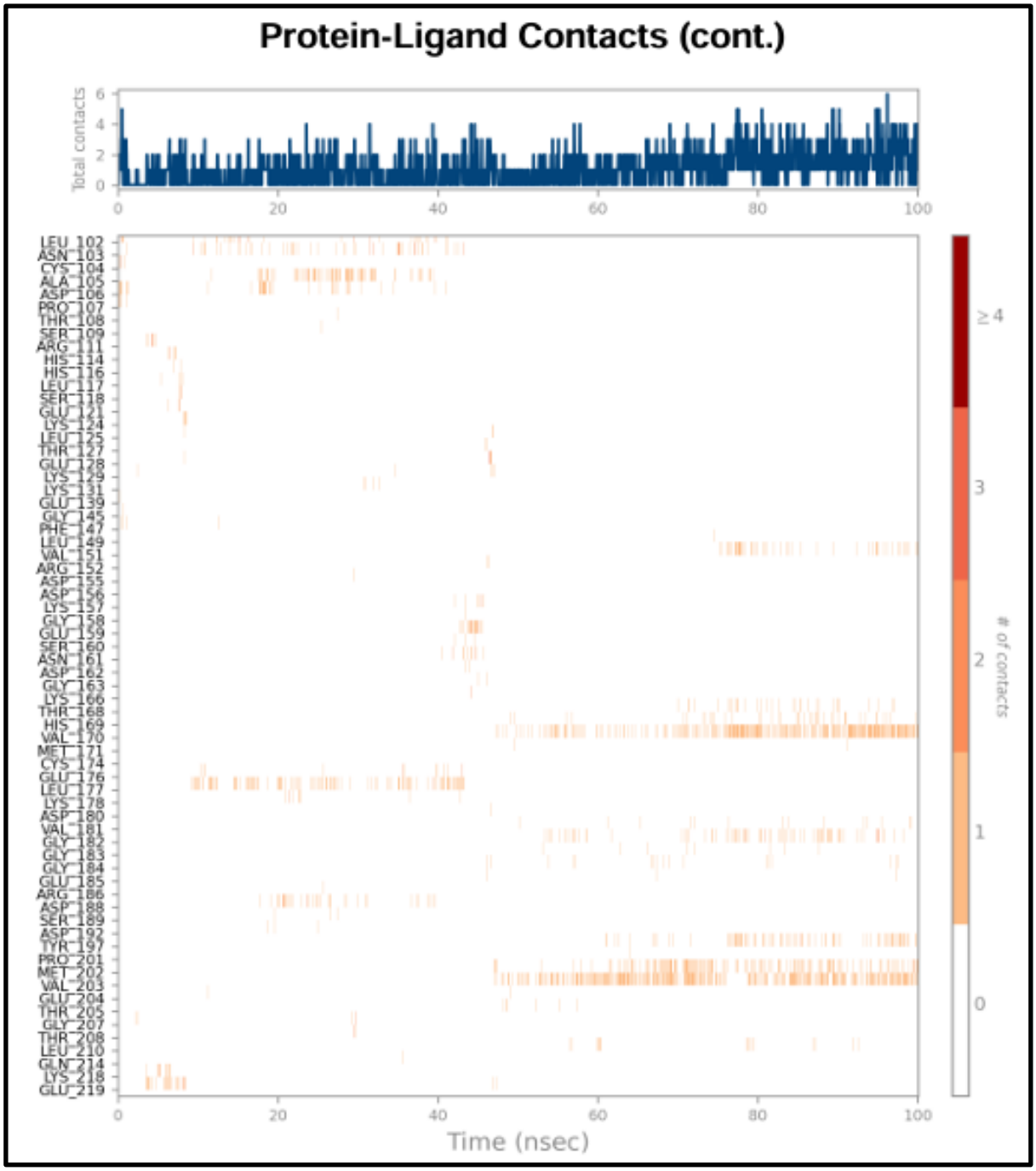

Figure 14: Protein Ligand Contacts of SHP2 (4JEG).

The **Figure 14**. represents the amino acid interactions between the protein SHP2 and *Berberine chloride*. This exhibits intermittent interaction profiling, which suggests secondary regulatory influence rather than strong inhibition.

6.3. Bar-graph representation of Protein-Ligand contacts:

This representation exhibits the interaction of each target protein with the ligand *Berberine chloride*, which exhibits the affinity between them.

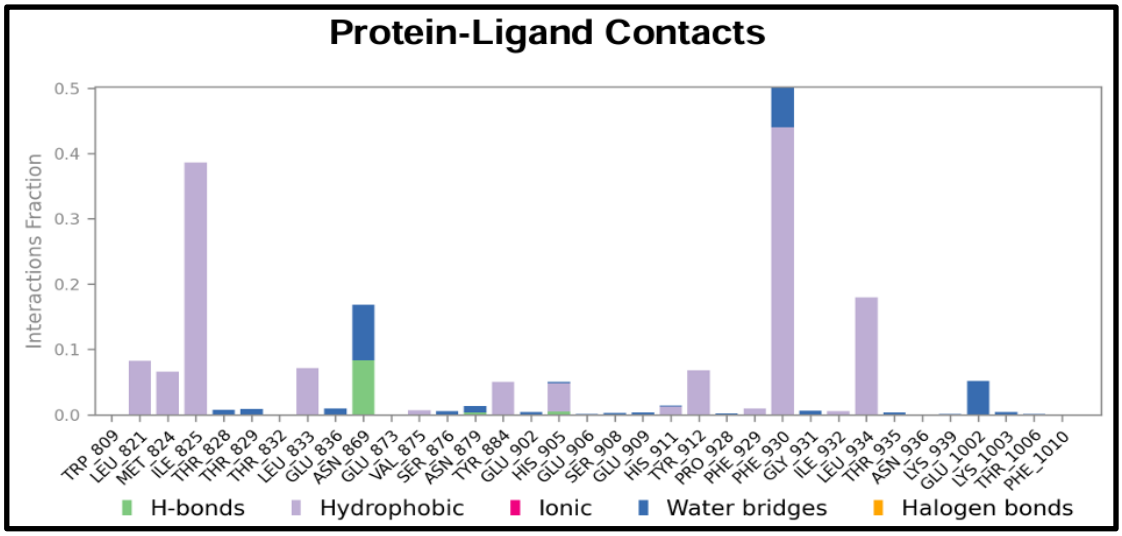

Figure 15: Graphical Representation of Protein-Ligand Contacts for SOS1 (6SFR).

The **Figure 15**. represents the bar graph of the contact residues between the protein SOS1 and the ligand *Berberine chloride*. This shows the low contact frequency and confirms the moderate affinity.

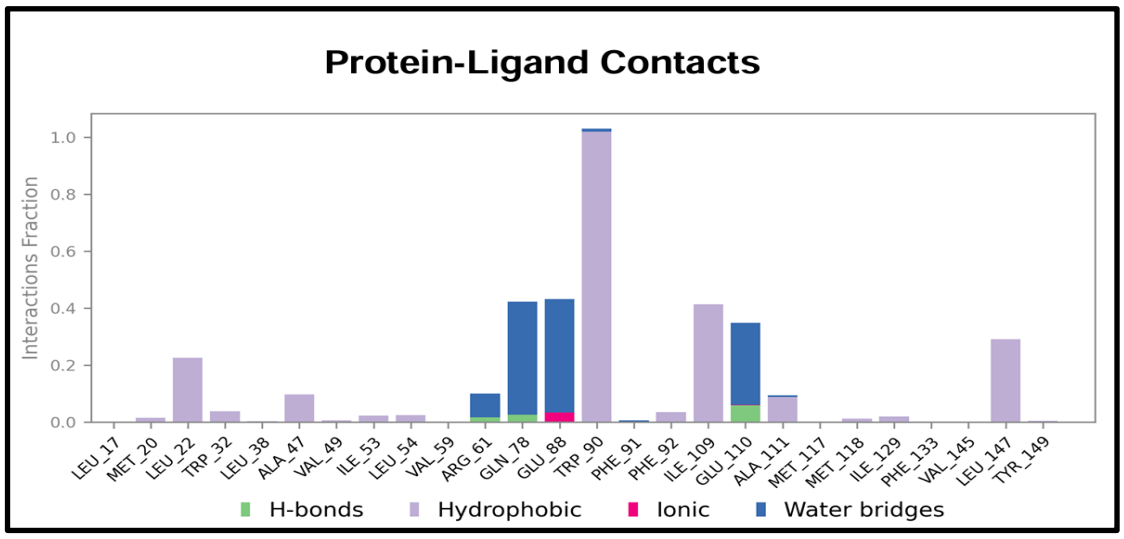

Figure 16: Graphical Representation of Protein-Ligand Contacts for PDE6D (5ML2).

The **Figure 16**. represents the bar graph of the contact residues between the chaperone PDE6D and the ligand *Berberine chloride*. These results again confirm the strongest and most stable interaction with high and persistent bar heights.

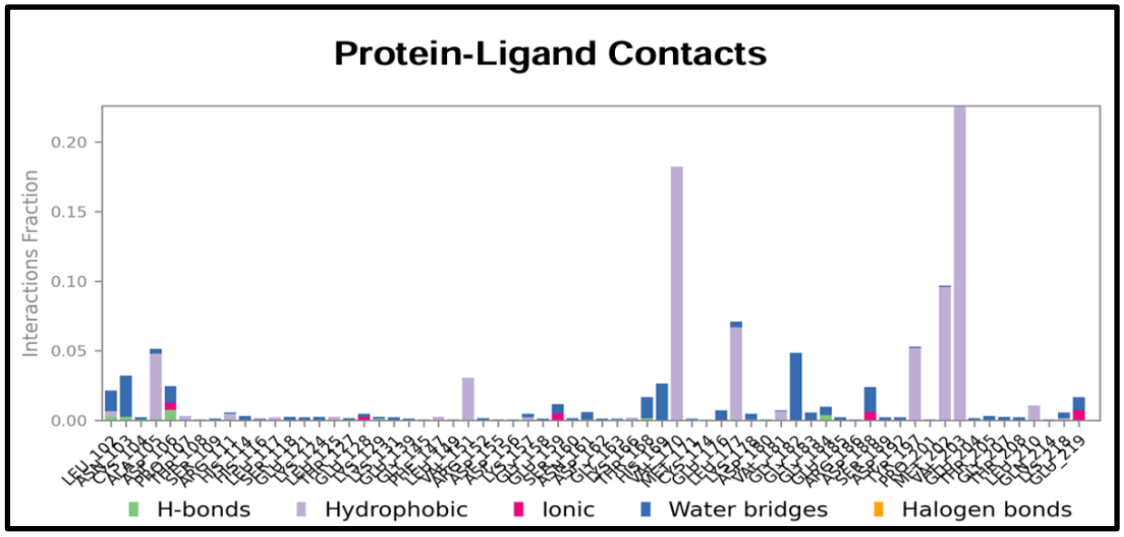

Figure 17: Graphical Representation of Protein-Ligand Contacts for SHP2 (4JEG).

Figure 17. represents the bar graph of the contact residues between the protein SHP2 and the ligand *Berberine chloride*. These results show moderate interactions with fluctuating intensity, which supports the weak docking but stable MD behaviour.

6.4. Ligand Properties:

The Ligand was subjected to a check for its internal properties for a time duration of 100 ns.

6.4.1. Root Mean Square Deviation (RMSD) of the Ligand:

RMSD of a ligand in relation to the reference conformation in ns. The frame below is used as the reference, and it is regarded as time *t=0.*

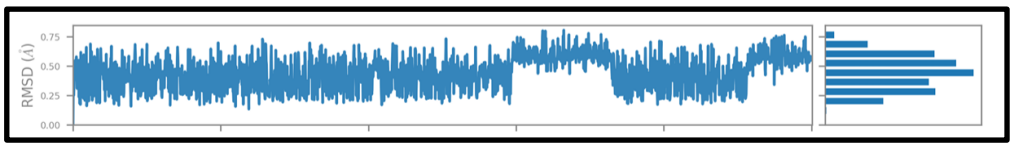

Figure 18 (a). Diagrammatic Representation of Ligand RMSD properties.

The Ligand RMSD confirms the strong structural retention across all the protein structures as represented in **Figure 18 (a).**

6.4.2. Radius of Gyration (rGyr) of the Ligand:

Evaluates a ligand's extendedness and is comparable to its primary moment of inertia.

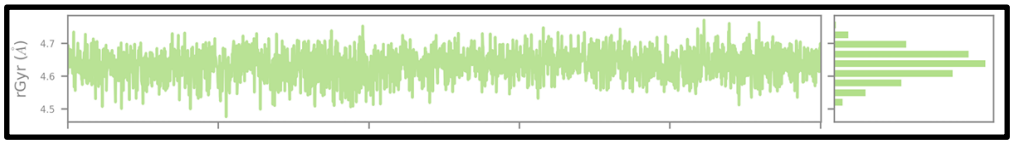

Figure 18 (b). Diagrammatic Representation of Ligand rGyr Properties.

These results confirm the steady throughout all simulations, and it maintains a compact and stable conformation as represented in **Figure 18 (b)**.

6.4.3. Intramolecular Hydrogen Bonds (intra HB):

This indicates how many internal hydrogen bonds a ligand molecule has.

Figure 18 (c). Diagrammatic Representation of Ligand's Intramolecular Hydrogen Bond.

This confirms the absence of Intra-HBs, which confirms that the ligand does not undergo internal collapse as represented in **Figure 18 (c)**.

6.4.4. Molecular Surface Area (MolSA):

Calculate the molecular surface using a 1.4 Å probe radius. A van der Waals surface area is equal to this value.

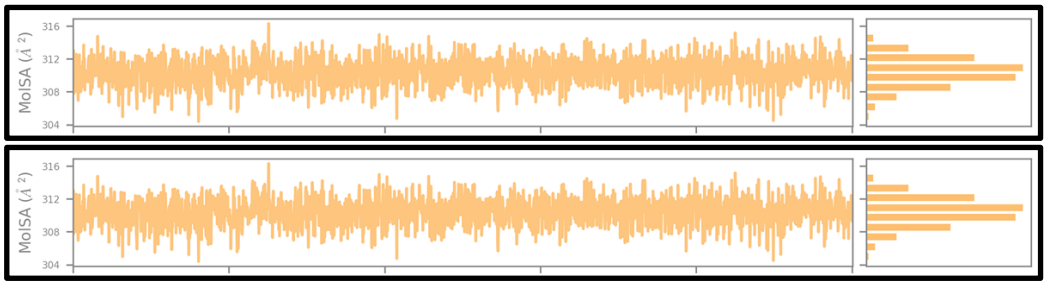

Figure 18 (d). Diagrammatic Representation of Ligand MolSA Properties.

The stable values of this representation reflect consistent exposure and fit inside the protein pockets as represented in **Figure 18 (d)**.

6.4.5. Solvent Availability Surface Area (SASA):

This allows a water molecule to access all of a molecule's information.

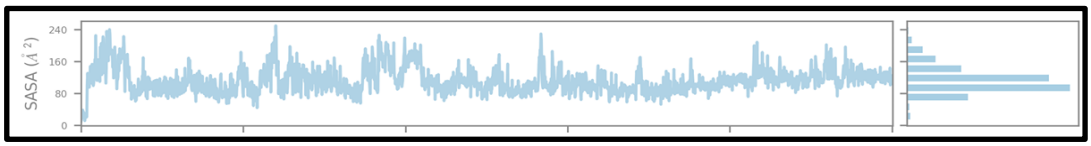

Figure 18 (e). Diagrammatic Representation of Ligand SASA Properties.

This shows the minimal fluctuation that indicates a stable solvation environment for the ligand as represented in **Figure 18 (e)**.

6.4.6. Polar Surface Area (PSA):

Only nitrogen and oxygen atoms contribute to a molecule's solvent-accessible surface area.

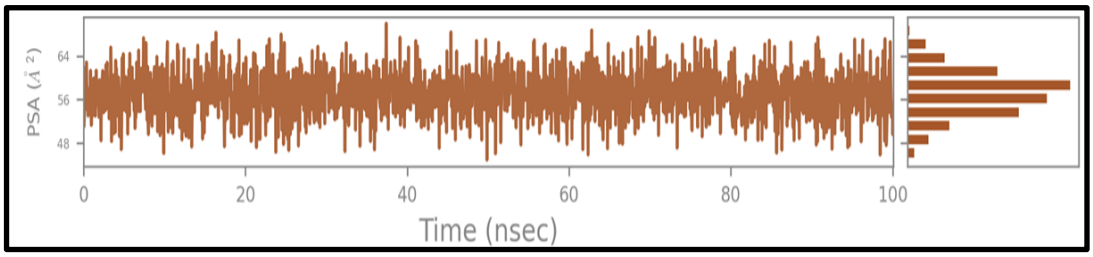

Figure 18 (f). Diagrammatic Representation of Ligand PSA Properties.

This represents the consistent PSA, which predicts the polarity-driven interactions across the trajectory as represented in **Figure 18 (f)**.

7. ADMET Results:

Absorption:

Model Name	**Predicted Value**	**Unit**
Water Solubility	-3.06	Numeric (log mol/L)
Caco2 permeability	0.88	Numeric (log Papp in 10-6 cm/s)
Intestinal absorption (human)	79.298	Numeric (% absorbed)
Skin Permeability	-2.622	Numeric (log Kp)
P-glycoprotein Substrate	Yes	Categorical (Yes/No)
P-glycoprotein I inhibitor	No	Categorical (Yes/No)
P-glycoprotein II inhibitor	Yes	Categorical (Yes/No)

Table 03: Representation of the Absorption results obtained from the pkCSM software.

The Absorption in **Table 03.** exhibits high human intestinal absorption with low solubility and P-gp substrate. This predicts bioavailability issues.

Distribution:

Model Name	**Predicted Value**	**Unit**
VDss (human)	0.385	Numeric log (L/kg)
Fraction Unbound (human)	0.291	Numeric (Fu)
BBB Permeability	0.241	Numeric (log BB)
CNS Permeability	-1.529	Numeric (log PS)

Table 04: Representation of the Distribution results obtained from the pkCSM software.

Metabolism:

Model Name	Predicted Value	Unit
CYP2D6 Substrate	No	Categorical (Yes/No)
CYP3A4 Substrate	Yes	Categorical (Yes/No)
CYP1A2 Inhibitor	Yes	Categorical (Yes/No)
CYP2C19 Inhibitor	No	Categorical (Yes/No)
CYP2C9 Inhibitor	No	Categorical (Yes/No)
CYP2D6 Inhibitor	No	Categorical (Yes/No)
CYP3A4 Inhibitor	No	Categorical (Yes/No)

Table 05: Representation of the Metabolism results obtained from the pkCSM software.

Table 05 represents the metabolism data of pkCSM. This shows potential metabolic interactions as a CYP3A4 substrate, and CYP1A2 inhibition was predicted.

Excretion:

Model Name	Predicted Value	Unit
Total Clearance	1.618	Numeric (log ml/min/kg)
Renal OCT2 Substrate	No	Categorical (Yes/No)

Table 06: Representation of the Excretion results obtained from the pkCSM software.

Table 06. confirms the normal clearance with no renal transporter risk.

Toxicity:

Model Name	Predicted Value	Unit
AMES Toxicity	Yes	Categorical (Yes/No)
Max. Tolerated Dose (Human)	0.027	Numeric (log mg/kg/day)
hERG I Inhibitor	No	Categorical (Yes/No)
hERG II Inhibitor	Yes	Categorical (Yes/No)
Oral Rat Acute Toxicity (LD 50)	2.458	Numeric (mol/kg)
Oral Rat Chronic Toxicity (LOAEL)	2.155	Numeric (log mg/kg bw/day)
Hepatotoxicity	Yes	Categorical (Yes/No)

Model Name	Predicted Value	Unit
AMES Toxicity	Yes	Categorical (Yes/No)
Skin Sensitisation	No	Categorical (Yes/No)
T. Pyriformis Toxicity	0.339	Numeric (log ug/L)
Minnow Toxicity	0.262	Numeric (log mM)

Table 07: Representation of the Toxicity results obtained from the pkCSM software.

Table 07. represents the toxicity prediction data in which AMES positive, predicted hepatotoxicity, and hERG II inhibition indicate the need for dose control and nano-formulation strategies.

Discussion:

The overall discussion suggests that KRAS remains one of the most challenging oncogenic drivers to target in NSCLC, which is mainly due to the absence of deep binding pockets and its high intrinsic affinity for GTP. Recent therapeutics have given a great breakthrough to target the upstream regulators of KRAS, which are included in our study: SOS1, SHP2, and the chaperone PDE6D. To check the target, we incorporated docking and MD simulations and ADMET prediction to evaluate the potential of the drug of interest.

The docking results revealed the most favourable binding partner of *Berberine chloride* PDE6D with a -7.9-docking score, binding with amino acids Glutamine, Isoleucine, and Tryptophan, which exhibits the highest binding affinity by forming stable hydrophobic and polar interactions. The moderate affinity exhibited by proteins SOS1 and SHP2 indicates secondary regulatory potential. The MD simulations were further strengthened. The PDE6D-*Berberine chloride* complex exhibits minimal fluctuations and better structural stability over 100 ns. Hence, with all these validations in the protein target, PDE6D can be targeted to regulate KRAS.

After validating the protein target, the ligand-based analyses, which included RMSD, rGyr, SASA, PSA, and MolSA, demonstrate *Berberine chloride* maintains structural integrity throughout the simulation. These analyses give a better standard to consider for inhibition development. The ADMET analysis of *Berberine* (BBR) was performed using the pkCSM web server. It demonstrated full compliance with Lipinski's rule of five, exhibiting a molecular weight of 371.82Da, LogP value of 0.1003, 4 hydrogen bond acceptors, and zero hydrogen bond donors, all together indicating drug likeness with no violation of the rule. BBR showed adequate intestinal absorption of 79.298%, exceeding the 70% threshold considered predictive of good oral bioavailability. BBR was identified as a P -glycoprotein (P-gp) substrate and gpII inhibitor, suggesting that the efflux-mediated mechanisms may partially limit its effective oral absorption in vivo. The predictive volume of distribution and a free fraction of 0.291 indicate moderate tissue partitioning with sufficient unbound drug available for pharmacological activity. The blood-brain barrier (BBB) permeability value of +0.241 suggests that blood-brain barrier penetration, which may be pharmacologically

relevant. The absence of inhibitory activity against CYP2C9, CYP2C19, CYP2D6, and CYP3A4 isoforms substantially limits the broader DDI liability of the compound. From a toxicological standpoint, BBR shows a positive AMES mutagenicity signal and predicted hepatotoxicity, which suggests experimental validation is needed before advancing to drug development. Basically, AMES toxicity depends on the amount and duration of drug intake, which is to be optimized through wet lab studies. Even Paclitaxel, which is an FDA-approved drug, shows AMES toxicity but has been optimized through dose and duration.

8. Future Perspectives:

The overall results of this paper give molecular insights into upstream regulators of KRAS that can be targeted through the MAPK pathway. The future of our work focuses on the reduction of drug usage and drug enhancement through nano-formulation. However, the in-silico approach gives only partial confirmation and cannot be completely reliable, as wet lab validation is needed for this study. There might be changes in the wet lab due to various external factors. This can be further considered for developing therapeutics for precision oncology, as mentioned in **Figure 19**.

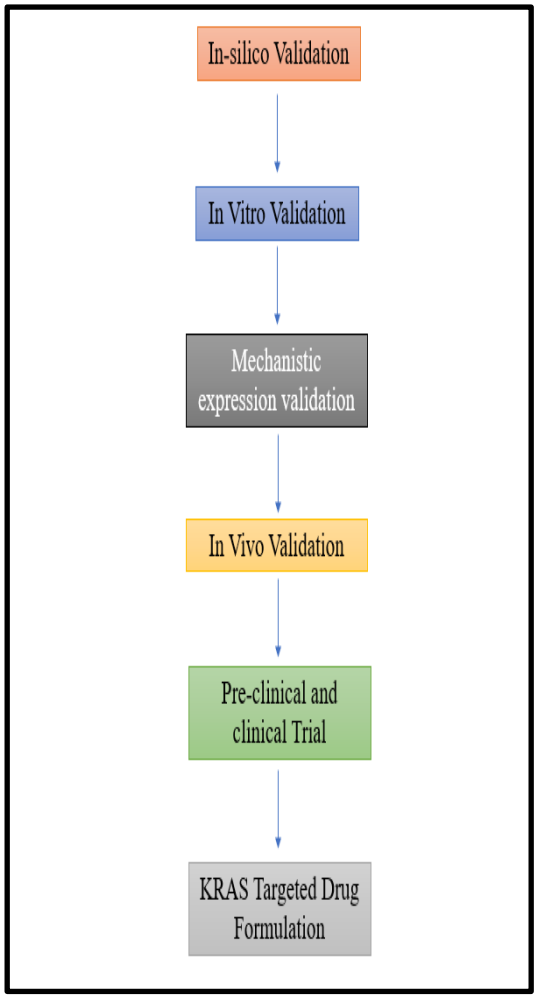

Figure 19. Diagrammatic Representation of Future Perspectives.

9. Conclusion:

This research work demonstrates that *Berberine chloride* exhibits a strong binding affinity and dynamic stability towards the key regulatory inhibitor PDE6D, which reveals its potential to modulate the KRAS activation through indirect upstream inhibition. The consideration of MD simulations for 100ns and molecular docking confirms the stable protein-ligand interactions with minimal deviations. Further down the studies with support for the ligand behavioural analyses, such as RMSD, rGyr,

SASA, and PSA, followed by ADMET profiling, suggest the acceptable drug-likeness and pharmacokinetic characteristics, with limitations primarily related to efflux and potential hepatotoxicity. Overall results propose the drug *Berberine chloride* as a promising natural compound, which can interrupt the KRAS regulatory signalling in lung adenocarcinoma through inhibition of PDE6D. This validates the PDE6D as a better binding target for *Berberine chloride* to treat KRAS-mutated NSCLC. As per our knowledge, there is no paper to date that potentially studies the interaction of the chaperone PDE6D and the ligand *Berberine chloride*.

References:

1. Kumar M, Sarkar A. Current therapeutic strategies and challenges in NSCLC treatment: A comprehensive review. Experimental oncology. 2022;44(1):7-16.
2. Frille A, Boeschen M, Wirtz H, Stiller M, Blaeker H, von Laffert M. TP53 co-mutations in advanced lung adenocarcinoma: comparative bioinformatic analyses suggest ambivalent character on overall survival alongside KRAS, STK11 and KEAP1 mutations. Frontiers in Oncology. 2024 Apr 22; 14:1357583.
3. Lv L, Liu Z, Liu Y, Zhang W, Jiang L, Li T, Lu X, Lei X, Liang W, Lin J. Distinct EGFR mutation pattern in patients with non-small cell lung cancer in Xuanwei region of China: a systematic review and meta-analysis. Frontiers in Oncology. 2020 Nov 2; 10:519073.
4. Nair A, Chakraborty S, Banerji LA, Srivastava A, Navare C, Saha B. Ras isoforms: signaling specificities in CD40 pathway. Cell Communication and Signaling. 2020 Jan 6;18(1):3.
5. Siegel RL, Miller KD, Fuchs HE, Jemal A. Cancer statistics, 2022. CA: a cancer journal for clinicians. 2022 Jan;72(1):7-33.
6. Prior IA, Hood FE, Hartley JL. The frequency of Ras mutations in cancer. Cancer research. 2020 Jul 15;80(14):2969-74.
7. Arauz RF, Byun JS, Tandon M, Sinha S, Kuhn S, Taylor S, Zingone A, Mitchell KA, Pine SR, Gardner K, Perez-Stable EJ. Whole-exome profiling of NSCLC among African Americans. Journal of Thoracic Oncology. 2020 Dec 1;15(12):1880-92.
8. Gregory MD, Ofosu-Asante K, Lazarte JM, Puente PE, Tawfeeq N, Belony N, Huang Y, Offringa IA, Lamango NS. Treatment of a mutant KRAS lung cancer cell line with polyisoprenylated cysteinyl amide inhibitors activates the MAPK pathway, inhibits cell migration and induces apoptosis. PloS one. 2024 Oct 22;19(10): e0312563.
9. Liu J, Kang R, Tang D. The KRAS-G12C inhibitor: activity and resistance. Cancer gene therapy. 2022 Jul;29(7):875-8.
10. Moore AR, Rosenberg SC, McCormick F, Malek S. RAS-targeted therapies: is the undruggable drugged? Nat Rev Drug Discov. 2020 Aug;19(8):533-552.
11. Wadhwa R, Paudel KR, Shukla S, Shastri M, Gupta G, Devkota HP, Chellappan DK, Hansbro PM, Dua K. Epigenetic therapy as a potential approach for targeting oxidative stress–induced non-small-cell lung cancer. Handbook of oxidative stress in cancer: Mechanistic aspects. 2021 Oct 14:1-6.
12. Mehta M, Malyla V, Paudel KR, Chellappan DK, Hansbro PM, Oliver BG, Dua K. Berberine loaded

liquid crystalline nanostructure inhibits cancer progression in adenocarcinomic human alveolar basal epithelial cells in vitro. Journal of Food Biochemistry. 2021 Nov;45(11): e13954.

13. Chen Q, Hou Y, Li D, Ding Z, Xu X, Hao B, Xia Q, Li M, Fan L. Berberine induces non-small cell lung cancer apoptosis via the activation of the ROS/ASK1/JNK pathway. Annals of Translational Medicine. 2022 Apr;10(8):485.
14. Doroudian M, MacLoughlin R, Poynton F, Prina-Mello A, Donnelly SC. Nanotechnology based therapeutics for lung disease. Thorax. 2019 Oct 1;74(10):965-76.
15. Battu SK, Repka MA, Maddineni S, Chittiboyina AG, Avery MA, Majumdar S. Physicochemical characterization of berberine chloride: a perspective in the development of a solution dosage form for oral delivery. Aaps Pharmscitech. 2010 Sep;11(3):1466-75.
16. Chen J, Huang X, Tao C, Wang L, Chen Z, Li X, Zeng Q, Ma M, Zhang R, Wu Z. Berberine chloride suppresses non-small cell lung cancer by deregulating Sin3A/TOP2B pathway in vitro and in vivo. Cancer chemotherapy and pharmacology. 2020 Jul;86(1):151-61.
17. Malyla V, De Rubis G, Paudel KR, Chellappan DK, Hansbro NG, Hansbro PM, Dua K. Berberine nanostructures attenuate ß-catenin, a key component of epithelial-mesenchymal transition in lung adenocarcinoma. Naunyn-Schmiedeberg's archives of pharmacology. 2023 Dec;396(12):3595-603.
18. Zhou S, Zhang D, Li J, Zhao J, Wang G, Zhang Y, Bai Y, Chen D, Wu H. Landscape of RAS variations in 17,993 pan-cancer patients identified by next-generation sequencing. Pathology & Oncology Research. 2020 Oct;26(4):2835-7.
19. Wahl SG, Dai HY, Emdal EF, Berg T, Halvorsen TO, Ottestad AL, Lund-Iversen M, Brustugun OT, Førde D, Paulsen EE, Donnem T. The prognostic effect of KRAS mutations in non-small cell lung carcinoma revisited: a Norwegian multicentre study. Cancers. 2021 Aug 26;13(17):4294.
20. Lee J, Tan AC, Zhou S, Yoon S, Liu S, Masuda K, Hayashi H, Batra U, Kim DW, Goto Y, Tan SH. Clinical characteristics and outcomes in advanced KRAS-mutated NSCLC: a multicenter collaboration in Asia (ATORG-005). JTO Clinical and Research Reports. 2022 Jan 1;3(1):100261.
21. Hofmann MH, Gmachl M, Ramharter J, Savarese F, Gerlach D, Marszalek JR, Sanderson MP, Kessler D, Trapani F, Arnhof H, Rumpel K. BI-3406, a potent and selective SOS1–KRAS interaction inhibitor, is effective in KRAS-driven cancers through combined MEK

inhibition. Cancer discovery. 2021 Jan 1;11(1):142-57.

22. Canon J, Rex K, Saiki AY, Mohr C, Cooke K, Bagal D, Gaida K, Holt T, Knutson CG, Koppada N, Lanman BA. The clinical KRAS (G12C) inhibitor AMG 510 drives anti-tumour immunity. Nature. 2019 Nov 7;575(7781):217-23.

23. Hallin J, Engstrom LD, Hargis L, Calinisan A, Aranda R, Briere DM, Sudhakar N, Bowcut V, Baer BR, Ballard JA, Burkard MR. The KRASG12C inhibitor MRTX849 provides insight toward therapeutic susceptibility of KRAS-mutant cancers in mouse models and patients. Cancer discovery. 2020 Jan 1;10(1):54-71.

24. Janes MR, Zhang J, Li LS, Hansen R, Peters U, Guo X, Chen Y, Babbar A, Firdaus SJ, Darjania L, Feng J. Targeting KRAS mutant cancers with a covalent G12C-specific inhibitor. Cell. 2018 Jan 25;172(3):578-89.

25. Li T, Kikuchi O, Zhou J, Wang Y, Pokharel B, Bastl K, Gokhale P, Knott A, Zhang Y, Doench JG, Ho ZV. Developing SHP2-based combination therapy for KRAS-amplified cancer. JCI insight. 2023 Feb 8;8(3): e152714.

26. Perrotti D, Neviani P. Protein tyrosine phosphatase SHP2: a pleiotropic target at the interface of cancer and its microenvironment. Cancer Res. 2023;83(20):3393-3403.

27. Hao HX, Wang H, Liu C, Kovats S, Velazquez R, Lu H, Pant B, Shirley M, Meyer MJ, Pu M, Lim J. Tumor intrinsic efficacy by SHP2 and RTK inhibitors in KRAS-mutant cancers. Molecular cancer therapeutics. 2019 Dec 1;18(12):2368-80.

28. Zheng W, Yang Z, Song P, Sun Y, Liu P, Yue L, Lv K, Wang X, Shen Y, Si J, Zhang X. SHP2 inhibition mitigates adaptive resistance to MEK inhibitors in KRAS-mutant gastric cancer through the suppression of KSR1 activity. Cancer Letters. 2023 Feb 28; 555:216029.

29. Samatar AA, Poulikakos PI. Targeting RAS–ERK signalling in cancer promises and challenges. Nat Rev Drug Discov. 2014;13(12):928-942.

30. Kaya P, Schaffner-Reckinger E, Manoharan GB, Vukic V, Kiriazis A, Ledda M, Burgos Renedo M, Pavic K, Gaigneaux A, Glaab E, Abankwa DK. An improved PDE6D inhibitor combines with sildenafil to inhibit KRAS mutant cancer cell growth. Journal of Medicinal Chemistry. 2024 May 17;67(11):8569-84.

31. Wang L, Wei D, Li S, Jiang S. Advances in biomarkers of resistance to KRAS mutation-targeted inhibitors. Discover Oncology. 2025 Oct 8;16(1):1834.

32. Yelland T, Garcia E, Parry C, Kowalczyk D, Wojnowska M, Gohlke A, Zalar M, Cameron K, Goodwin G, Yu Q, Zhu PC. Stabilization of the ras: Pde6d complex is a novel strategy to inhibit ras signaling. Journal of Medicinal Chemistry. 2022 Feb 2;65(3):1898-914.

33. Isermann T, Sers C, Der CJ, Papke B. KRAS inhibitors: resistance drivers and

combinatorial strategies. Trends in cancer. 2025 Feb 1;11(2):91-116.

34. Martín-Gago P, Fansa EK, Klein CH, Murarka S, Janning P, Schürmann M, Metz M, Ismail S, Schultz-Fademrecht C, Baumann M, Bastiaens PI. A PDE6δ-KRas inhibitor chemotype with up to seven H-bonds and picomolar affinity that prevents efficient inhibitor release by Arl2. Angewandte Chemie. 2017 Feb 20;129(9):2463-8.

35. Hofmann MH, Gmachl M, Ramharter J, Savarese F, Gerlach D, Marszalek JR, Sanderson MP, Kessler D, Trapani F, Arnhof H, Rumpel K. BI-3406, a potent and selective SOS1–KRAS interaction inhibitor, is effective in KRAS-driven cancers through combined MEK inhibition. Cancer discovery. 2021 Jan 1;11(1):142-57.

36. Sha F, Gencer EB, Georgeon S, Koide A, Yasui N, Koide S, Hantschel O. Dissection of the BCR-ABL signaling network using highly specific monobody inhibitors to the SHP2 SH2 domains. Proceedings of the National Academy of Sciences. 2013 Sep 10;110(37):14924-9.

37. National Center for Biotechnology Information. PubChem compound summary.

38. Schrödinger Release 2025-4: LigPrep, Schrödinger, LLC, New York, NY, 2025.

39. Yang Y, Yao K, Repasky MP, Leswing K, Abel R, Shoichet BK, Jerome SV. Efficient exploration of chemical space with docking and deep learning. Journal of Chemical Theory and Computation. 2021 Sep 30;17(11):7106-19.

40. Robertson MJ, van Zundert GC, Borrelli K, Skiniotis G. GemSpot: a pipeline for robust modeling of ligands into cryo-EM maps. Structure. 2020 Jun 2;28(6):707-16.

41. Bowers KJ, Chow E, Xu H, Dror RO, Eastwood MP, Gregersen BA, Klepeis JL, Kolossvary I, Moraes MA, Sacerdoti FD, Salmon JK. Scalable algorithms for molecular dynamics simulations on commodity clusters. In Proceedings of the 2006 ACM/IEEE Conference on Supercomputing 2006 Nov 11 (pp. 84-es).

42. Pires DE, Blundell TL, Ascher DB. pkCSM: predicting small-molecule pharmacokinetic and toxicity properties using graph-based signatures. Journal of medicinal chemistry. 2015 May 14;58(9):4066-72.

Declarations:

Ethical Approval: Not applicable as this study does not involve any human or animal trial, it involves only in silico tools.

Consent for Publication: The published manuscript has been published with the consent and approval of all the mentioned authors.

Availability of data and materials: All the data analysed in this study were from previously published literature and from the results obtained during conducting the research. The figures were created using PowerPoint by the authors themselves and taken from the obtained data from the software, and do not require any permissions for their use.

Competing Interests: The authors declare that they have no competing interests.

Funding: This research did not receive any specific grant for this publication.

Author Contributions:

Mr. Arjun KR – Conceptualization, Literature Review, Writing the Original draft, Data Collection.

Dr. Shakeel Ahmed Adhoni – Review of literature, Conceptualization.

Dr.Ullas Prasanna S – Conceptualization

Dr. Baburao Gaddala – Literature review and reviewing the manuscript.

Dr. Shailasree Shekhar – Reviewing the manuscript

Mr. Jeyarish V – In silico work, data analysis, conceptualization, and interpretation.

Ms. Varshitha BR – Literature Review and Writing the Original draft.

Ms. Vindhya M – Writing the Original Draft and Review.

Dr. Hemalatha Modugapalem - Reviewing the manuscript and Communication for publishing.

Dr. Kanthesh M Basalingappa – Supervision, review, and final approval of manuscript.

AI Enclosure: No AI was used for data generation, image creation, content, or data analysis. Only language editing tools for minor grammatical corrections, such as Grammarly was used.

Research Originality Statement: We, the authors, declare that the published manuscript and data are original and have not been published elsewhere.

Plagiarism Statement: We, the authors, confirm that the data is free from plagiarism and have been acknowledged throughout the paper wherever necessary with standard Academic Practices.

Acknowledgement: The Authors thank JSS Academy of Higher Education and Research for their constant support.